Wavefunctions from energies: Applications in simple potentials

View Online   Export Citation   CrossMark

Darío M. Mitnik[1,a] (iD) and **Santiago A. H. Mitnik**[2]

AFFILIATIONS

[1] Instituto de Astronomía y Física del Espacio, CONICET–UBA, Buenos Aires, Argentina
[2] Escuela de Política y Gobierno, UNSAM, Buenos Aires, Argentina

[a] Author to whom correspondence should be addressed: dmitnik@df.uba.ar

ABSTRACT

A remarkable mathematical property—somehow hidden and recently rediscovered—allows obtaining the eigenvectors of a Hermitian matrix directly from their eigenvalues. This opens the possibility to get the wavefunctions from the spectrum, an elusive goal of many fields in physics. Here, the formula is assessed for simple potentials, recovering the theoretical wavefunctions within machine accuracy. A striking feature of this eigenvalue–eigenvector relation is that it does not require knowing any of the entries of the working matrix. However, it requires the knowledge of the eigenvalues of the minor matrices (in which a row and a column have been deleted from the original matrix). We found a pattern in these sub-matrix spectra, allowing us to get the eigenvectors analytically. The physical information hidden behind this pattern is analyzed.

Published under license by AIP Publishing. https://doi.org/10.1063/5.0011115

I. INTRODUCTION

Recently,[1] precise perturbative calculations of neutrino oscillation probabilities yielded a surprising result: given the eigenvalues of the Hamiltonian and its minor sub-matrices, it is possible to write down all the probabilities by a quite simple expression. In a following two page paper, the authors[2] described and proved this eigenvector–eigenvalue identity (1), which is the subject of the present work. Despite its simplicity and possible implications, the identity was not broadly well known. Lately, it achieved a blaze of publicity after a popular article[3] reported the unexpected relationship between the eigenvalues and eigenvectors in the neutrino oscillation calculations. The authors of Ref. 2 rewrote the paper adding thirty pages with several proofs of the identity, together with a discussion about its complicated history in the literature and the reasons why so few people were aware of it. They also showed that the equation appeared in different references, being independently rediscovered in diverse fields. In most cases, the papers were weakly connected, lacking in significant propagation of citations.

The *eigenvector–eigenvalue identity*[2] relates the eigenvectors v_i of an $n \times n$ Hermitian matrix H, with its eigenvalues $\lambda_1, \lambda_2, \ldots, \lambda_n$. In this work, it is slightly modified as follows:

$$|v_{j,i}|^2 \prod_{k=1;k\neq i}^{n} (\lambda_i - \lambda_k) = \prod_{k=1}^{n-1} \left(\lambda_i - \lambda_k^{(j)} \right), \tag{1}$$

where v_{ji} is the jth component of the normalized eigenvector v_i associated with the eigenvalue λ_i. The eigenvalues $\lambda_1^{(j)}, \lambda_2^{(j)}, \ldots, \lambda_{n-1}^{(j)}$ correspond to the minor M_j of H, formed by removing the jth row and column.

Identity (1) has many remarkable aspects to discuss. We can mention many positive and very promising issues. First, note that at no point does one ever actually need to know any of the entries of the matrix to calculate its eigenvectors. From the physical point of view, this can be very useful in systems in which the eigenvalues are obtained by measurements. The most direct application could be the recovering of the electronic densities from the experimental spectra, which is, perhaps, the holy grail of physical chemistry. Second, it can lead to the development of new numerical methods to diagonalize large matrices faster and more efficiently. The standard computer routines use much more memory and resources if the eigenvectors are needed solely in place of the eigenvalues.

However, these two advantages have some weaknesses. Indeed, the values of the original matrix H are not needed, but since expression (1) involves the minors M_j, this statement is not completely straight. It will be undisputed only if the minor's eigenvalues $\lambda_i^{(j)}$ are available, without the explicit knowledge of the matrix elements. From the numerical point of view, the new algorithms do not seem to be competitive, unless for very large matrices. The reason is that for every eigenvector v_i, all the eigenvalues $\lambda_k^{(j)}$ of each minor M_j are needed. Thus, the algorithm requires to obtain all the eigenvalues of $n-1$ different matrices, which will result in a much more costly way to solve an eigenproblem.

In the present work, all these aspects are examined. First, we prove the eigenvector–eigenvalue identity for the solution of the corresponding Schrödinger equation for simple one-dimensional potentials. The wavefunctions obtained by direct diagonalization and by using expression (1) are compared for harmonic oscillators, Coulombic potentials, and the infinite potential well. Then, the spectra of the minor matrices are analyzed. We found that these eigenvalues are not randomly scattered, else they behave systematically, forming a pattern that could be described analytically. Finally, a deep analysis of the minor's eigenvalues $\lambda^{(j)}$ for the simplest potential (the infinite potential well) leads us to understand the origin of this singular behavior, which could be useful for the calculation of eigenvectors of other potentials.

II. ASSESSMENT OF THE EIGENVALUE–EIGENVECTOR IDENTITY

To corroborate expression (1) in physical problems, we will validate it first, in simple potential problems, solving the one-dimensional Schrödinger equation

$$\hat{H}(x)\, v_i(x) = \lambda_i\, v_i(x), \tag{2}$$

where

$$\hat{H} = -\frac{1}{2}\frac{d^2}{dx^2} + V(x). \tag{3}$$

We choose the most commonly studied simple potentials, say, the harmonic oscillator,

$$V(x) = V_{\text{HO}}(x) \equiv \frac{1}{2}\omega^2\,(x - x_0), \tag{4}$$

the Coulomb potential,

$$V(x) = V_{\text{C}}(x) \equiv -\frac{Z}{x}, \tag{5}$$

and the infinite potential well,

$$V(x) = V_{\text{W}}(x) \equiv \begin{cases} V_0 & \text{for } x \leq L \\ \infty & \text{for } x > L. \end{cases} \tag{6}$$

For each potential, the corresponding Schrödinger equation was approximated in first-order finite differences, resulting in tridiagonal matrices. First, the full Hamiltonians have been diagonalized by using standard computational packages,[4] getting the eigenvectors v and eigenvalues λ. Next, we successively construct the minor matrices M_j, deleting from the full Hamiltonian matrix the jth row and column. In that way, the corresponding $\lambda^{(j)}$ eigenvalues have been obtained. Finally, Eq. (1) is used to get the "reconstructed" eigenvalues. The operations involved in this rebuilding require some care. The order of the operations is important, and in addition, it is better to add logarithms than to multiply terms having different orders of magnitudes. One of the principal numerical advantages of the proposed approach resides in the fact that the matrices are not needed but only their eigenvalues. Therefore, we also take care to exploit that, performing the calculation in a particular sequence, in which only one minor's eigenvalues are stored in memory, at any step.

For all these potentials and many different Hamiltonian sizes, the reconstructed results agree with the original eigenvectors within machine precision. Thus, the first conclusion reached in the present work is that for any number n of points used in the numerical grid, the eigenvalue–eigenvector identity can be considered numerically exact.

Of course, there is a drawback in expression (1), and it is the requirement of the calculation of the eigenvalues for n different matrices, which, in general, takes more computational efforts than the direct diagonalization of an $n \times n$ matrix. The algorithm can be significantly improved if one can find some relationship between the original eigenvalues λ_i and the corresponding minor's eigenvalues $\lambda_i^{(j)}$. To this end, we first plot these eigenvalues to see if they follow some identifiable behavior. We show, in Fig. 1, the $\lambda_i^{(j)}$ values corresponding to an infinite potential well $V_{\text{W}}(x)$ [Eq. (6)] of size $L = 20$ a.u. and amplitude $V_0 = 0$, calculated with a numerical grid having $n = 33$ points. From Fig. 1, we cannot get any useful information because of the similarities among the $\lambda_i^{(j)}$ eigenvalues for any minor matrix j.
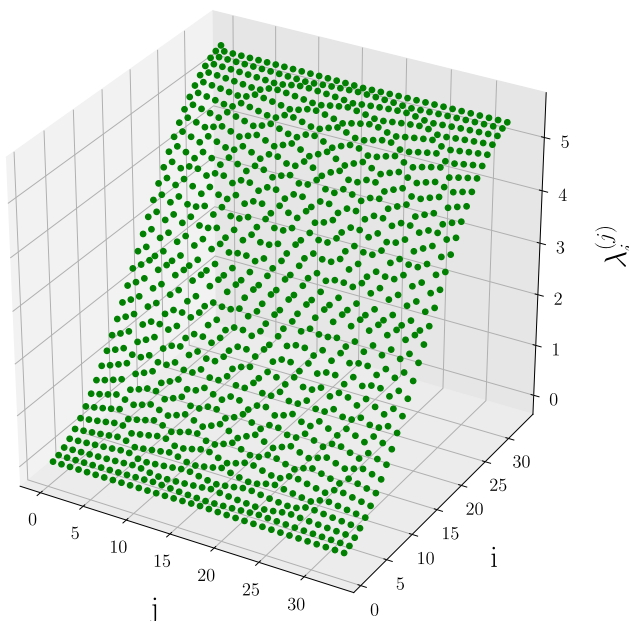
FIG. 1. Eigenvalues $\lambda_i^{(j)}$ of the minor matrices M_j for the V_W–Hamiltonian corresponding to the infinite potential well.

For a better representation, we define and plot, in Fig. 2, the differences $D(i,j) \equiv \lambda_i - \lambda_i^{(j)}$, which could be helpful to understand the meaning of the minor's eigenvalues.

These differences have been calculated for three different potentials: an infinite potential well, a Coulomb potential, and a harmonic oscillator potential. An unexpected regular pattern appears in the three cases, encouraging the search for analytical expressions capable to represent these values.
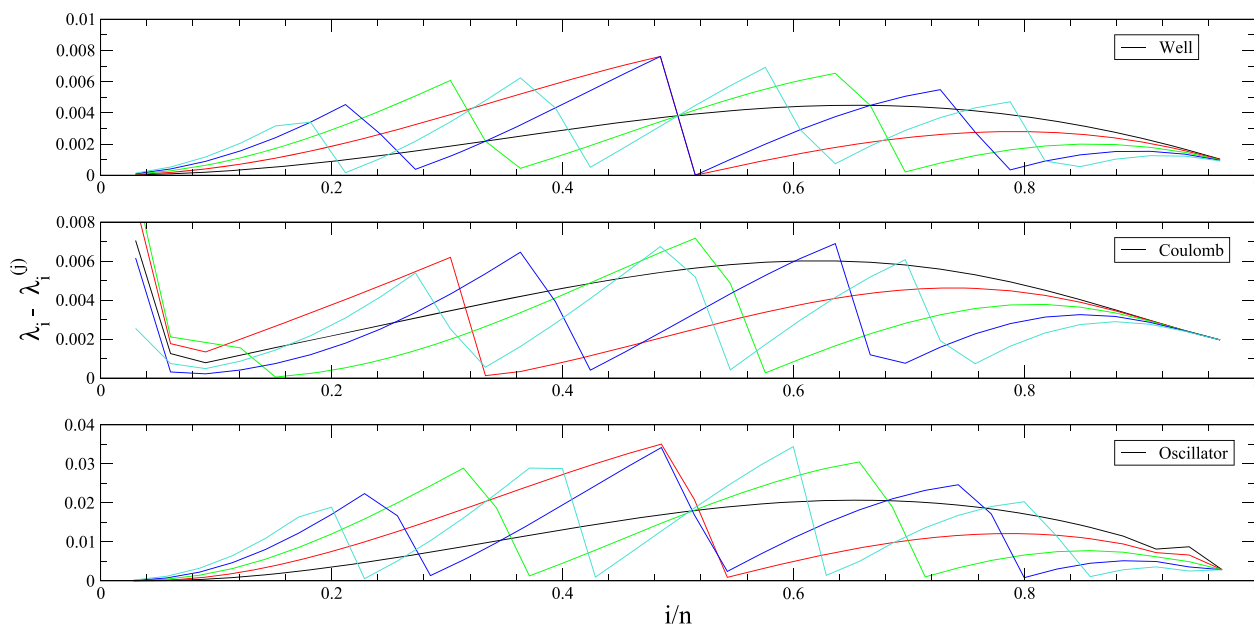
FIG. 2. Differences between the full Hamiltonian eigenvalues λ_i and the eigenvalues $\lambda_i^{(j)}$ of the minor matrices M_j for the infinite potential well $V_W(x)$, the Coulomb potential $V_C(x)$, and the harmonic oscillator potential $V_{HO}(x)$.

III. ANALYTICAL EXPRESSION FOR THE MINOR'S EIGENVALUES

Although the curves shown in Fig. 2 suggest the possibility to find analytical functions to represent the minor's eigenvalues, this task is not straightforward. Let us analyze the eigenvalues of the minor matrices for the infinite potential well $V_W(x)$, which seems to be the potential having the most regular behavior. It is important to stress that we are dealing with the numerical solutions of a first order finite-difference approximation, which are different than the exact solutions. We will first attempt to understand the state of affairs in the numerical solutions and will treat the exact solutions in further works (see a brief discussion in Appendix B).

For the first minor matrix M_1, the differences $D(i, 1)$ are arranged in a smooth curve, which is easily approximated, as is shown in Fig. 3, by the expression

$$D(i, 1) \equiv \lambda_i - \lambda_i^{(1)} \approx A_1\, i\, \sin\left(\frac{\pi i}{a_1}\right), \tag{7}$$

where a_1 is very close to n, the number of points in the numerical grid.

The analytic approximation is more difficult for the next minor matrix M_2. Here (see Fig. 4), there are two different noticeable regions d, and each one should be approximated separately, i.e.,

$$D^{(d)}(i, j) \equiv \lambda_i - \lambda_i^{(j)}\,|_{i \in d} \approx A_j^d\, i\, \sin\left(\frac{\pi i}{a_j^d}\right). \tag{8}$$

For $j = 2$, the first coefficient $a_2^1 = a_1 \approx n$, but for the second half of the eigenvalues ($d = 2$), the appropriate value is $a_2^2 \approx \frac{n}{2}$ (formal expressions for a_j^d are given in Appendix A). The complications related to pursuing an understanding of the behavior of the minor's eigenvalues do not end here. We found that the size of the Hamiltonian also affects how $D(i, 2)$ are approximated. Let us see these values for a case in which the number of points in the numerical grid is even. Figure 5 shows the differences between the eigenvalues of a Hamiltonian matrix with $n = 34$ points (in place of the previous values shown in Fig. 4, where $n = 33$). Here, the differences for the first 16 eigenvalues $D^{(1)}(i, 2)$ are approximated with (8) using a set of parameters A_j^d and a_j^d and the last 16 eigenvalues $D^{(2)}(i, 2)$ are approximated by using another set, as in the previous case. However, the difference $D(17, 2) = \lambda_{17} - \lambda_{17}^{(2)}$ does not belong to either of both curves. Surprisingly, we found that this value agrees exactly with the difference obtained for the first minor, which is $D(17, 1) = \lambda_{17} - \lambda_{17}^{(1)}$.

More intricate is the approximation for the M_3 minor's eigenvalues ($j = 3$). We start the analysis with a Hamiltonian matrix having $n = 35$ points. As is shown in Fig. 6, we need to establish three different regions d, where the size of each one is pretty near $1/3$ (see Appendix A). Since 34 is not divisible by 3, we do not know beforehand how many points i belong to each region d. We found that approximation (8) works well for the three ranges on considering 11 points belonging to the first and last regions and 12 points belonging to the middle region. The corresponding parameters a are roughly $a_3^1 \approx n$, $a_3^2 \approx \frac{2n}{3}$, and $a_3^3 \approx \frac{n}{3}$. As pointed out before, this distribution is particular for a given Hamiltonian size. The $n = 33$ case is illustrated in Fig. 7. Here, 10 eigenvectors can be fitted very well with (8) for each region d. We run into trouble at two points corresponding to $i = \frac{n}{3}$ and $i = \frac{2n}{3}$. As shown in Fig. 7, the same unexpected property found before holds for this case: for these points, the eigenvalue differences for M_3 coincide exactly with the corresponding values of the first minor M_1. Nevertheless, the picture
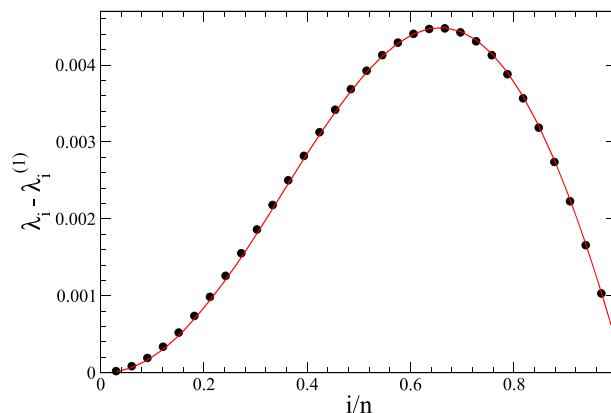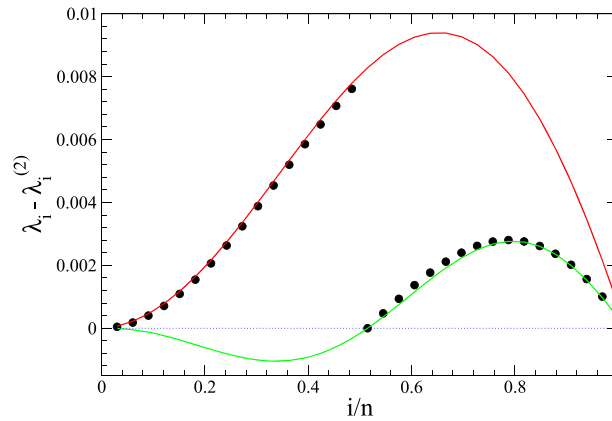

FIG. 3. Differences $\lambda_i - \lambda_i^{(1)}$ for the minor matrix M_1 for the infinite potential well V_W–Hamiltonian. Points: values obtained by direct diagonalization. Solid curve: analytic approximation.

FIG. 4. Differences $\lambda_i - \lambda_i^{(2)}$ for the minor matrix M_2. Points: values obtained by direct diagonalization. Solid curve: analytic approximation. The size of the V_W–Hamiltonian matrix is $n = 33$.

is different for $n = 34$, as is shown in Fig. 8. Here, the first and last regions hold 10 points, the central region holds 11 points, and in addition, two values lie outside these curves. Now, these values agree exactly with those corresponding to M_2.

In conclusion, the eigenvalue differences $D^{(d)}(i, j)$ follow the general behavior given in Eq. (8), in which the width coefficients

$$a_j^d \approx \frac{n}{j}(j - d + 1). \tag{9}$$

However, it seems very difficult to assign a simple formula for each minor index j, for each region d, and for any number of points n.

We emphasize that expression (9) is approximate. An accurate fitting for a values can be done, requiring a lot of work, since adjustments must be done to generalize it for every number of points n. These corrections are small and will not be significant for large matrices. However, establishing the number of points assigned to each sector d is not straightforward since it depends on the number of points n and varies for each minor index j. Assigning a wrong number of points to a particular region accumulates enormous errors in the reconstruction formula (1), turning any approximation of D useless. Furthermore, there are many problematic points k that do not belong to any of the regions d. The $D(k, j)$ differences for these points agree with the values calculated for other minors $D(k, p)$, where the minor index p also depends on j and the number of points n. We found the analytical expression that relates these indices,

$$p_n^{(j)} = \mathrm{mod}(n + 1 - j, j). \tag{10}$$
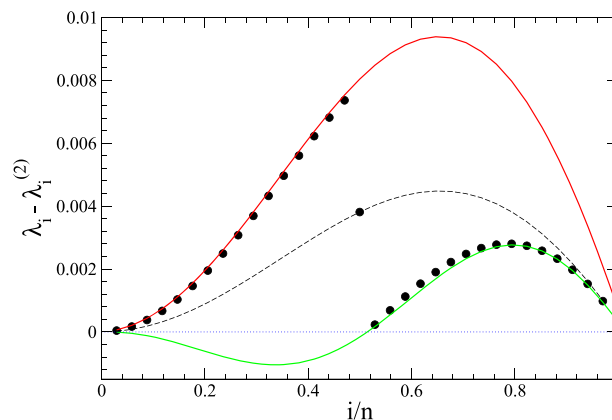
FIG. 5. Differences $\lambda_i - \lambda_i^{(2)}$ for the minor matrix M_2 for a V_W–Hamiltonian matrix with $n = 34$ points. Points: values obtained by direct diagonalization. Solid curve: analytic approximation. Dashed curve: differences $\lambda_i - \lambda_i^{(1)}$.
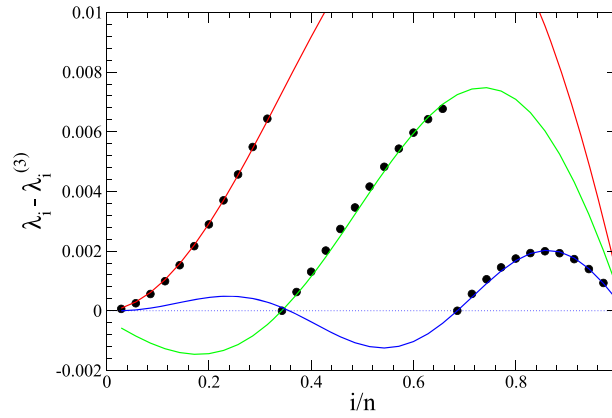
FIG. 6. Differences $\lambda_i - \lambda_i^{(3)}$ for the minor matrix M_3 for a V_W–Hamiltonian matrix with $n = 35$ points.
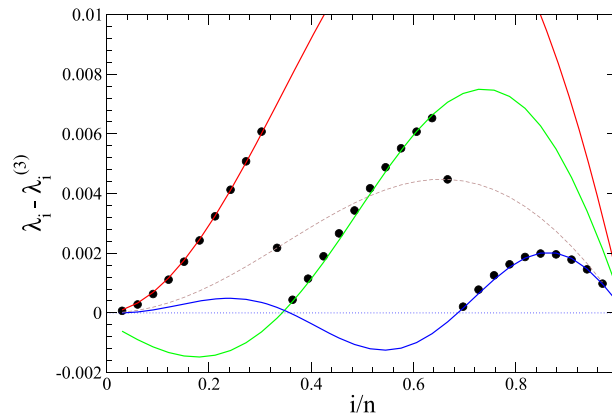

FIG. 7. Differences $\lambda_i - \lambda_i^{(3)}$ for the minor matrix M_3 for a V_W–Hamiltonian matrix with $n = 33$ points. Dashed curve: $\lambda_i - \lambda_i^{(1)}$.
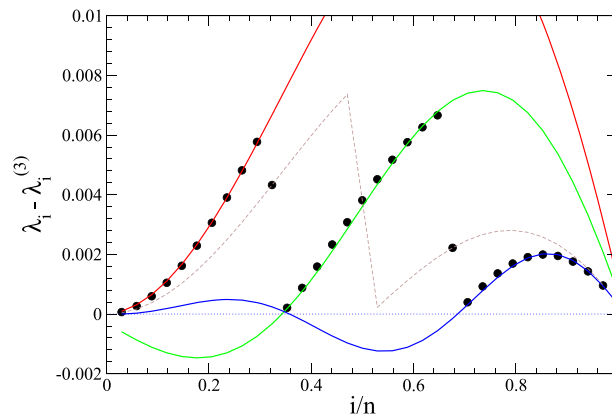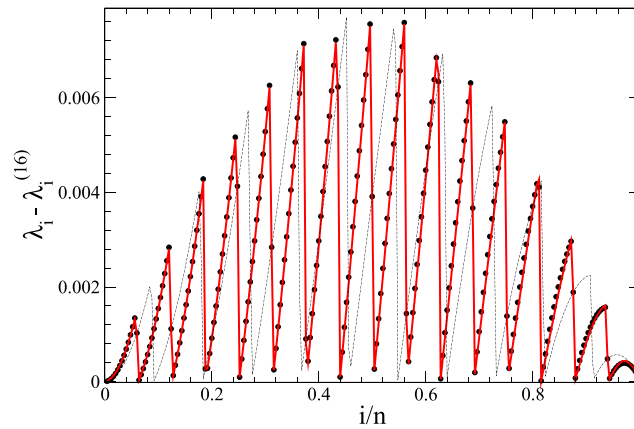

FIG. 8. Differences $\lambda_i - \lambda_i^{(3)}$ for the minor matrix M_3 for a V_W–Hamiltonian matrix with $n = 34$ points. Dashed curve: $\lambda_i - \lambda_i^{(2)}$.

FIG. 9. Differences $\lambda_i - \lambda_i^{(16)}$ for the minor matrix M_{16} for a V_W–Hamiltonian matrix with $n = 250$ points. Dashed curve: $\lambda_i - \lambda_i^{(11)}$.

Taking all these aspects into consideration, we can reproduce all the D values and thus all the eigenvalues $\lambda_i^{(j)}$ belonging to all the minor matrices M_j for any Hamiltonian size n. As an example, we illustrate, in Fig. 9, the eigenvalue differences $D(i, 16) = \lambda_i - \lambda_i^{(16)}$ for the minor matrix M_{16} and for a Hamiltonian matrix with $n = 250$ points. All the points k that are not fitted with the curves represented in solid lines have exactly the values $D(k, 11)$ corresponding to the minor matrix M_{11} (dashed curves), in agreement with our findings, since $p = \mathrm{mod}(235, 16) = 11$.
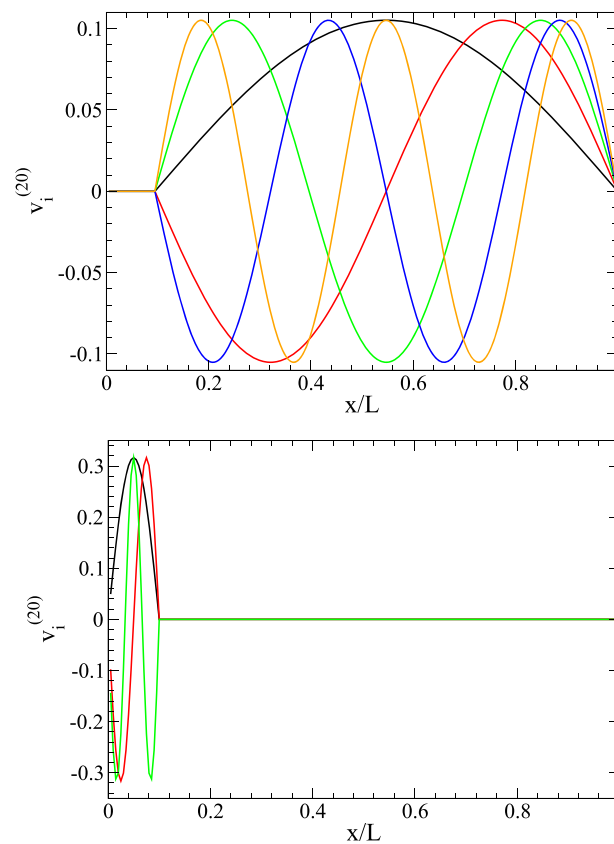
FIG. 10. Upper part: first eigenvectors $v_i^{(20)}$ for the minor matrix M_{20} for a V_W–Hamiltonian matrix with $n = 200$ points. Lower part: eigenvectors $v_{10}^{(20)}$, $v_{20}^{(20)}$, and $v_{30}^{(20)}$.

IV. PHYSICAL INTERPRETATION OF THE MINOR'S EIGENVALUES

Having decoded the startling pattern conformed by the minor's eigenvalues, many questions remain open. The behavior discovered is particular to the infinite potential well. From Fig. 2, it is reasonable to conjecture about the existence of similar relationships on the other potentials. All the eigenvalues have been calculated numerically. A question that arises is whether the same pattern holds also for the exact analytical results. The most important issue to solve is the possibility to recognize a physical meaning in our findings. Perhaps, understanding this matter could help answer the other questions.

The first physical realization of the eigenvector–eigenvalue identity was done by Voss and Balloon.[5] They showed that one-dimensional arrays of coupled resonators, described by square matrices with real eigenvalues, provide simple physical systems where this formula can be applied in practice. The subsystems consist of arrays with the jth resonator removed. Thus, from their spectra alone, the oscillation modes of the full system can be obtained.

Concerning the infinite potential well, the physical meaning of the removal of the first row and column is very simple: it conforms another infinite potential well whose width decreases from L to $L - \Delta x$, where Δx is the numerical mesh size. The same potential may be thought of as an infinite well of size L, with an additional infinite wall located at Δx. Accordingly, the removal of the jth row and column means an infinite potential well with an infinite wall at $x = j\Delta x$. As an example, we plot the first eigenvectors of the submatrix M_{20}, for an infinite potential well represented by $n = 200$ points, in Fig. 10. In the relative coordinates, it means that an infinite wall is present at $x/L = 0.1$. As is shown in Fig. 10, the first eigenvectors correspond to the eigenvectors of an $L - L/10$ infinite potential well. We also have to consider the other potential well of size $L/10$, which, for this particular case, has eigenvalues coincident with the full Hamiltonian spectra for every $i = 10$ function. The lower part of Fig. 10 shows the eigenvalues $v_{10}^{(20)}$, $v_{20}^{(20)}$, and $v_{30}^{(20)}$ having the same energy as v_{10}, v_{20}, and v_{30} from the full Hamiltonian.

V. CONCLUSIONS

The eigenvalue–eigenvector identity expresses a curious and surprising relationship between the eigenvector of a matrix and the eigenvalues of its minors. It can be very useful from the numerical point of view, encouraging the study of new techniques to solve large eigenproblems. In general, it is much simpler and faster to calculate the eigenvalues than the eigenvectors. Moreover, for very large matrices, the memory storage requirement for the standard eigenvector solver can lead to serious problems, which could be overcome by this approach. A critical element to strengthening the use of the identity is the ability to avoid the calculation of the eigenvalues of all the minor matrices.

In this work, we first tested the eigenvalue–eigenvector identity on different systems. The formula has been used to numerically reconstruct the eigenvectors of simple one-dimensional Hamiltonians. Using only the eigenvalues of the minor matrices, the formula reproduces the eigenvectors within machine precision even for large cases. In most cases, the eigenvalue λ_i is close to the $\lambda_i^{(j)}$ value. However, analyzing their differences $D(i, j) = \lambda_i - \lambda_i^{(j)}$, we found systematic patterns, allowing us to analytically extract the minor's eigenvectors without diagonalizing all the submatrices.

To understand the patterns, we focused our study on the infinite potential well. Elucidating the behavior of the differences $D(i, j)$ is not straightforward since they depend on the eigenvalue index i, on the minor index j, and also on the number n of points in the numerical grid representing the Hamiltonian. We found that, indeed, it is possible to find an analytical expression for $D(i, j)$ and, therefore, for all $\lambda_i^{(j)}$. The existence of regular patterns suggests that some hidden information about the eigenvectors of the full Hamiltonian is buried under the minor matrices' eigenvalue structure. A crucial aspect to understand this information is to find the physical reasons that generate those patterns. For the case studied here, the minor matrix represents a clear physical case that consists of the same Hamiltonian but with an infinite wall located at the point corresponding to the index j. The generalization to other potentials in 3 dimensions and for real scenarios can be a matter of further interesting development.

APPENDIX A: ANALYTICAL EXPRESSION FOR THE APPROXIMATION FORMULAS

In the first-order approximation, the numerical eigenvalues λ_i of the one dimension infinite potential well are related to the eigenvalues $\lambda_i^{(j)}$ of the minor submatrix M_j in the following way. Let us define a variable

$$x \equiv \frac{i}{n}, \tag{A1}$$

where i is the eigenvalue index and n is the number of grid points representing the eigenvectors. Numerically, an infinite potential well represented by an n-point Hamiltonian has n different eigenvalues; therefore, $x \in \{0, 1\}$. The eigenvalue differences $D(i, j) = \lambda_i - \lambda_i^{(j)}$ have

been found to cluster in j different sections, where the size of each of them is approximately n/j. More precisely, each section begins at a point

$$x_{0_j}^{(d)} = \frac{d-1}{j}\left(1 + \frac{1}{n}\right). \tag{A2}$$

It is worth noting that for the infinite potential well, the x_{0_j} points correspond to the nodes of the jth eigenvector.

The argument of the sin functions in Eq. (8) has a wavelength proportional to a width of

$$a_d^{(j)} = 1 - x_{0_j}^{(d)} + \frac{1}{2n}. \tag{A3}$$

The differences can be approximated by the expression

$$D^{(d)}(i,j) = A_j^{(d)} \sin\left(\frac{x - x_{0_j}^{(d)}}{a_d^{(j)}}\pi\right)(x + \Delta^{(d)}). \tag{A4}$$

The parameter $\Delta^{(d)}$ is given as follows:

$$\Delta^{(d)} = \begin{cases} \dfrac{d}{2n} & \text{for } d < \dfrac{j}{2} \\ \dfrac{j - d + 2}{2n} & \text{for } \dfrac{j}{2} \le d < j - 1 \\ -\dfrac{1}{2n} & \text{for } d = j - 1, \end{cases} \tag{A5}$$

and the coefficients $A_j^{(1)} = j$ and $A_j^{(j-1)} = \frac{1}{j}$, and in any other case,

$$A_j^{(d)} = \frac{j}{d}\frac{\sin\left(\frac{d}{j}\pi\right)}{\sin\left(\frac{\pi}{j-d+1}\right)}. \tag{A6}$$

It is very important to identify the limits of every sector d: the initial eigenvalue index $i_{0_j}^{(d)}$, the last point $i_{b_j}^{(d)}$, and the points $k_j^{(d)}$ that lie outside each region d. For simplicity, let us drop the indices i and d in Eq. (A2), so every section is bounded by the range

$$x_0 \equiv \frac{d-1}{j}\left(1 + \frac{1}{n}\right) < x < x_b \equiv \frac{d}{j}\left(1 + \frac{1}{n}\right). \tag{A7}$$

The corresponding $(x \times n)$ values are not necessarily integer numbers. We define the indices i_0 and i_{b_z} as the integer part of $(x_0 \times n)$ and $(x_b \times n)$, respectively. Then, we designate the following quantities:

$$(x_1, x_2, x_3) \equiv \left(\frac{i_{b_z} - 1}{n}, \frac{i_{b_z}}{n}, \frac{i_{b_z} + 1}{n}\right). \tag{A8}$$

The index i_b is defined as

$$i_b = \begin{cases} i_{b_z} - 1 & \text{for } x_1 < x_b \le x_2 \\ i_{b_z} & \text{for } x_2 < x_b \le x_3. \end{cases} \tag{A9}$$

Every sector contains the eigenvalue indices between

$$i_0 + 1 \le i \le i_b - 1. \tag{A10}$$

As explained above, the value of $D(i_b, j)^{(d)}$ is calculated by using Eq. (10), i.e., the value corresponding to the index $k = i_b$ is $D(k,j)^{(d)} = D(k, j_p)^{(p)}$, where

$$p = \text{mod}(n + 1 - j, j) \text{ and}$$
$$j_p = \frac{i_b p}{n}. \tag{A11}$$

APPENDIX B: IMPLEMENTATION IN THE EXACT SOLUTIONS

Here, we will show how to proceed for the reconstruction of the exact wavefunctions (not the numerical solutions, as before). In addition, we need to get the eigenvectors of an infinite potential well using the eigenvector–eigenvalue identity. Expression (1) involves a product, so we must decide, first, how many points should be used in it. This decision also determines which minor matrices are included and their eigenvalues. As stated above, the minor matrix M_j represents the original Hamiltonian matrix with an infinite wall at the corresponding position x_j. This wall separates the potential in two regions, in our case in two infinite wells: one from 0 to x_j and the other from x_j to 1. To reconstruct the eigenvectors through the eigenvector–eigenvalue identity, one must be aware of appropriately intercalating the energies of both wells.

As an example, let us pick 10 terms in product (1) to reconstruct the eigenvectors of an infinite potential well having a width $L = 11$ a.u. The walls are located at $x_j = 1, 2, 3, \ldots, 9, 10$ a.u. For instance, for the minor M_4, we need to calculate the spectra for two wells: one having a width $L_1 = 7$ and the other with $L_2 = 4$. Their corresponding energies are

$$\epsilon_n^{(i)} = \frac{1}{2}\left(\frac{n_i \pi}{L_i}\right)^2. \tag{B1}$$

For the box having $L_2 = 7$ a.u., the lowest energies are $\epsilon_1^1 = 0.1007$, $\epsilon_2^1 = 0.4028$, and $\epsilon_3^1 = 0.9064$ a.u., and for $L_1 = 4$ a.u., the lowest energies are $\epsilon_1^2 = 0.3084$, $\epsilon_2^2 = 1.2337$, and $\epsilon_3^3 = 2.7758$ a.u. The ordered eigenvalues $\lambda_i^{(4)}$ are stated in Table I together with the other values. The rest of the eigenvalues are obtained by considering the symmetry of the potentials, i.e., $\lambda_i^{(6)} = \lambda_i^{(5)}$, $\lambda_i^{(7)} = \lambda_i^{(4)}$, $\lambda_i^{(8)} = \lambda_i^{(3)}$, $\lambda_i^{(9)} = \lambda_i^{(2)}$, and $\lambda_i^{(10)} = \lambda_i^{(1)}$.

Using these eigenvalues, the eigenvector–eigenvalue equation reproduces the eigenvectors (at the positions x_j), without normalization. The normalized results are shown in Fig. 11 for the first five eigenvalues, demonstrating that the identity can also be used for exact analytical cases.

TABLE I. Lowest eigenvalues λ_i for the infinite potential well having a width $L = 11$ a.u. and eigenvalues $\lambda_i^{(j)}$ of the corresponding minor M_j matrices. For each case, the quantum number n_i and the width of the corresponding well L_i used in Eq. (B1) are indicated.

|	$\lambda_1^{(j)}$ (L_i, n_i)	$\lambda_2^{(j)}$ (L_i, n_i)	$\lambda_3^{(j)}$ (L_i, n_i)	$\lambda_4^{(j)}$ (L_i, n_i)	$\lambda_5^{(j)}$ (L_i, n_i)	$\lambda_6^{(j)}$ (L_i, n_i)	$\lambda_7^{(j)}$ (L_i, n_i)	$\lambda_8^{(j)}$ (L_i, n_i)	$\lambda_9^{(j)}$ (L_i, n_i)
H	0.0408 (11,1)	0.1631 (11,2)	0.3671 (11,3)	0.6525 (11,4)	1.0196 (11,5)	1.4682 (11,6)	1.9984 (11,7)	2.6101 (11,8)	3.3035 (11,9)
M_2	0.0493 (9,1)	0.1974 (9,2)	0.4441 (9,3)	0.7896 (9,4)	1.2337 (2,1)	1.7765 (9,5)	2.4181 (9,6)	3.1583 (9,7)	3.9972 (9,8)
M_3	0.0609 (8,1)	0.2437 (8,2)	0.5483 (3,1)	0.9748 (8,3)	1.2337 (8,4)	1.5231 (8,5)	2.1932 (3,2)	2.9853 (8,6)	3.8991 (8,7)
M_4	0.1007 (7,1)	0.3084 (4,1)	0.4028 (7,2)	0.9064 (7,3)	1.2337 (4,2)	1.6114 (7,4)	2.5178 (7,5)	2.7758 (4,3)	3.6256 (7,6)
M_5	0.1371 (6,1)	0.1974 (5,1)	0.5483 (6,2)	0.7896 (5,2)	1.2337 (6,3)	1.7765 (5,3)	2.1932 (6,4)	3.1583 (5,4)	3.4269 (6,5)
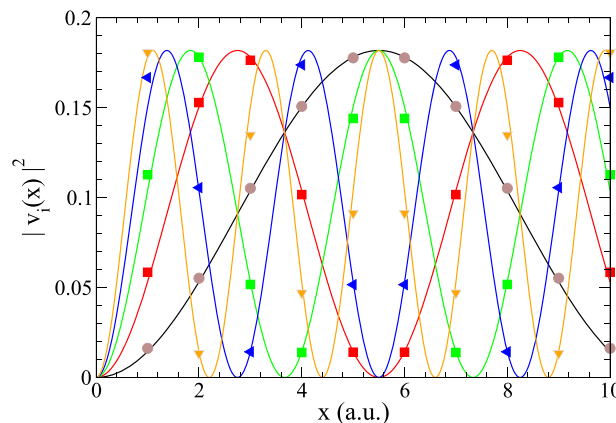
FIG. 11. First 5 exact eigenvalues $v_i(x)$ corresponding to an infinite potential well having a width $L = 11$ a.u. The curves represent $|v_i(x)|^2$. The points are the $|v_{ji}|^2$ values, calculated through the eigenvalue–eigenvector identity (1) (normalized).

DATA AVAILABILITY

The data that support the findings of this study are available from the corresponding author upon reasonable request.

REFERENCES

[1] P. B. Denton, S. J. Parke, and X. Zhang, "Neutrino oscillations in matter via eigenvalues," Phys. Rev D **101**, 093001 (2020).

[2] P. B. Denton, S. J. Parke, T. Tao, and X. Zhang, "Eigenvectors from eigenvalues: A survey of a basic identity in linear algebra," arXiv:1908.03795 [math.RA] (2019).

[3] N. Wolcholver, "Neutrinos lead to unexpected discovery in basic math," Quanta Mag. (2019), https://www.quantamagazine.org/neutrinos-lead-to-unexpected-discovery-in-basic-math-20191113.

[4] LAPACK, Linear Algebra PACKage, http://www.netlib.org/lapack/.

[5] H. U. Voss and D. J. Ballon, Phys. Rev. Res. **2**, 012054(R) (2020).